Electronic Supplementary Material (ESI) for Journal of Materials Chemistry A.

Supporting Information

Highly Active Mixed-Valent MnO_x Spheres Constructed by Nanocrystals as Efficient Catalyst for Long-life Li-O_2 Batteries

Sanpei Zhang,[‡, §] *Zhaoyin Wen,*[*,‡, §] *Yang Lu,*[‡, §] *Xiangwei Wu,*[‡] *and Jianhua Yang*[‡,§]

[‡] *CAS Key Laboratory of Materials for Energy Conversion*, *Shanghai Institute of Ceramics, Chinese Academy of Sciences, Shanghai 200050, P. R. China*

*E-mail: zywen@mail.sic.ac.cn

[§] *University of Chinese Academy of Sciences, Beijing 100049, P. R. China*

Contents

1. XRD pattern of the Mn-glycerate precursor

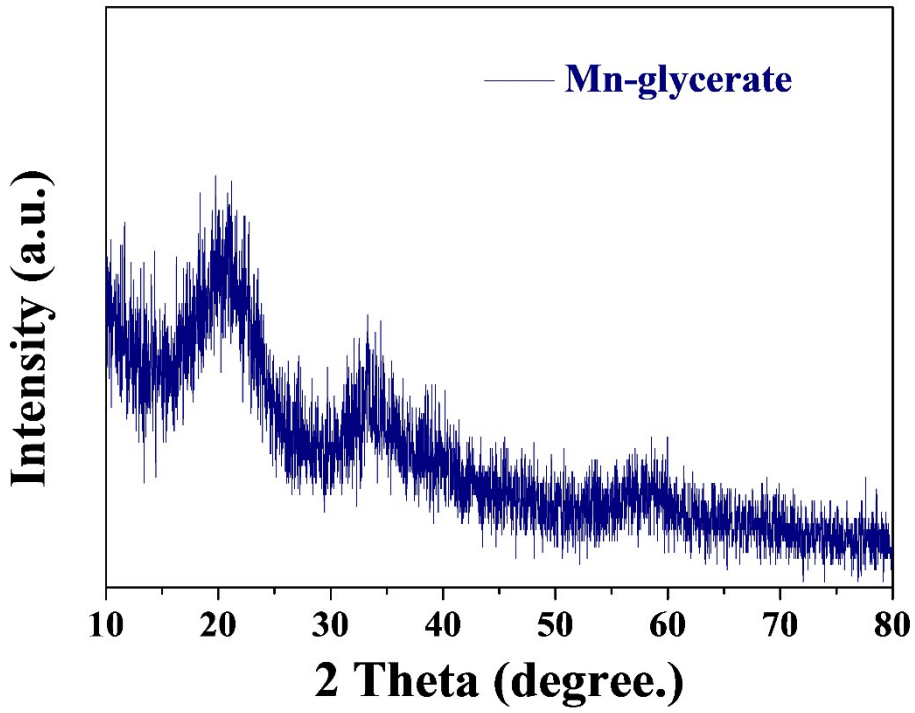

Figure S1. XRD patterns of the Mn-glycerate precursor.

2. Core photoelectron binding energies of various manganese oxides

Table S1. Core photoelectron binding energies of various manganese oxides.[1, 2]

Oxides	Photoelectron peak binding energy (eV)	
	$2p_{3/2}$	$2p_{1/2}$
MnO	640.9	653.0
Mn_3O_4	641.7	653.3
Mn_2O_3	641.8	653.6
MnO_2	652.4	654.0

Reference

1. J. Foord, R. Jackman and G. Allen, *Philosophical Magazine A*, 1984, **49**, 657-663.
2. G. Allen, S. Harris, J. Jutson and J. Dyke, *Appl Surf Sci*, 1989, **37**, 111-134.

3. XPS and EDX results of atomic content of various element in the as-prepared MnO_x spheres

Table S2. Atomic content of various element in the as-prepared MnO_x spheres

	Mn (%)	O (%)	C (%)
XPS	35.93	62.08	1.99
EDX	37.85	59.13	3.02
Average	**36.89**	**60.61**	

4. SEM and TEM images of Mn-glycerate spheres

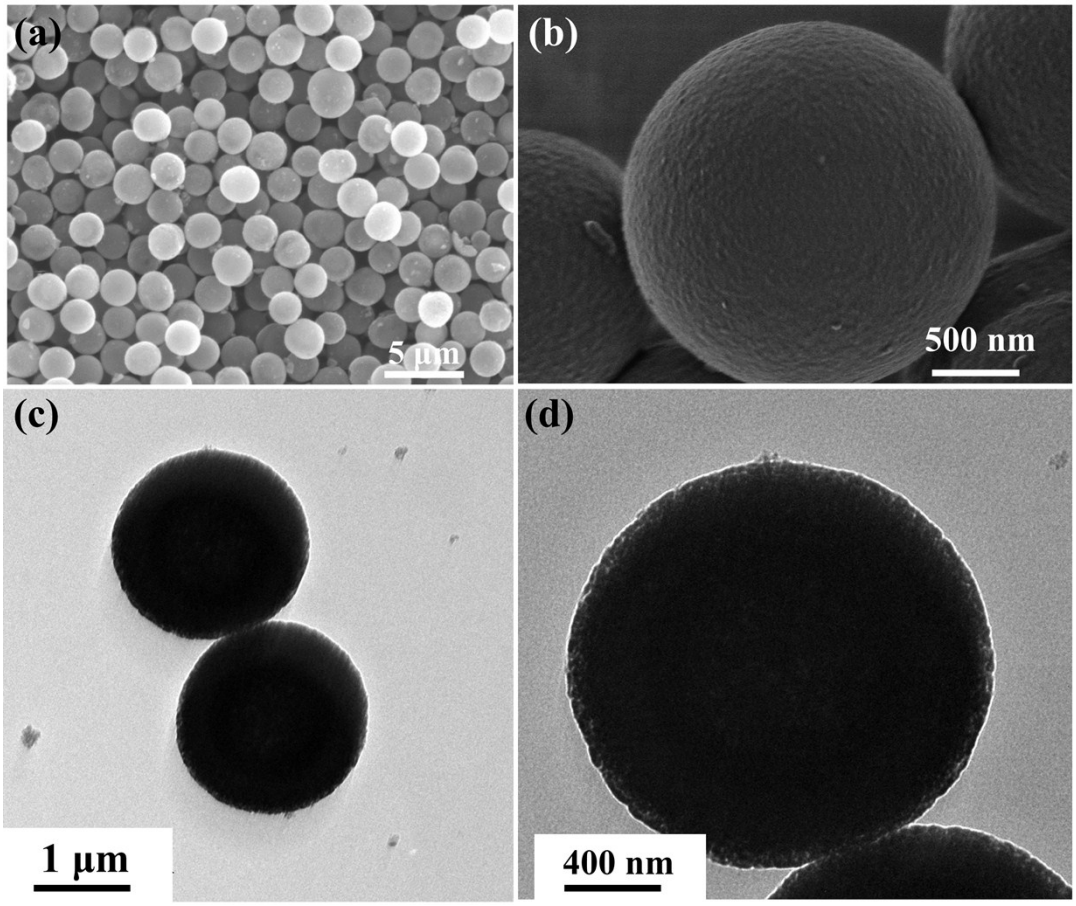

Figure S2. SEM and TEM images of the Mn-glycerate spheres.

5. Elemental mapping images of the mixed-valent MnO_x spheres

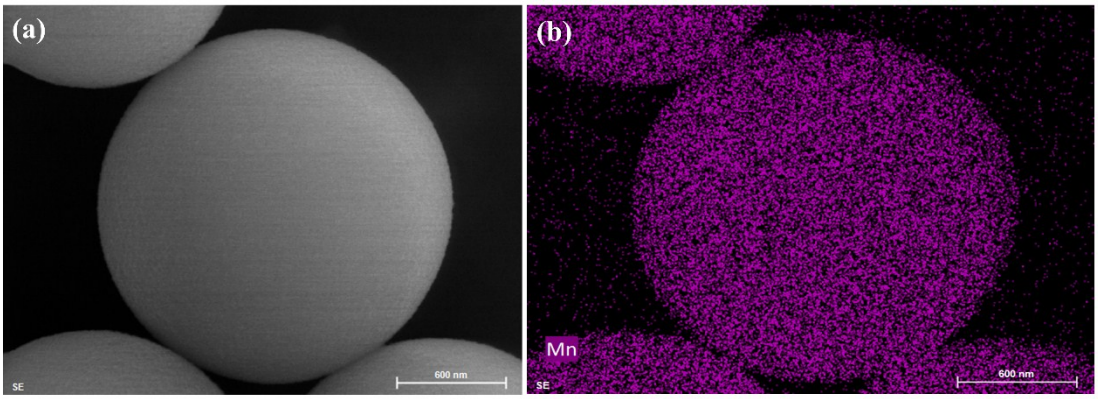

Figure S3. The dark-field scanning SEM image and corresponding elemental mapping image of the mixed-valent MnO_x spheres.

6. EDX spectra of the mixed-valent MnOx spheres

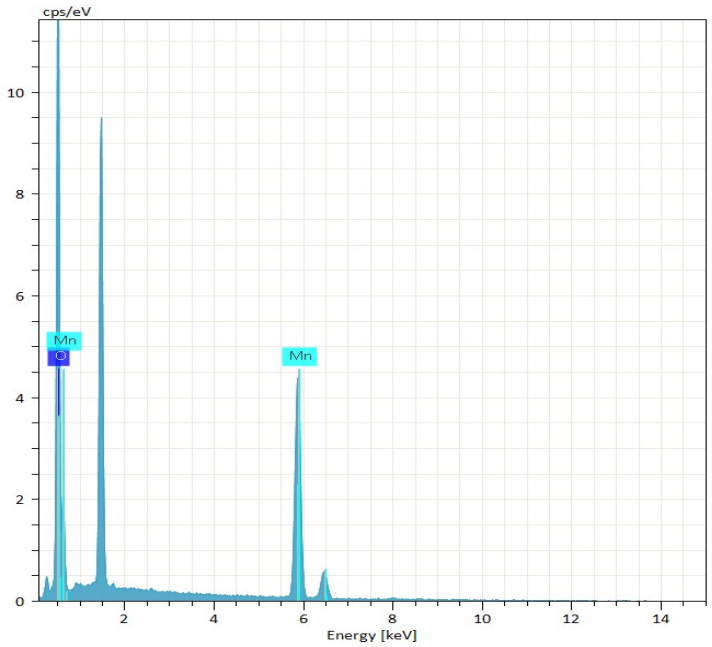

Figure S4. EDX spectra of the highly active mixed-valent MnO_x spheres.

7. Electrochemical performance of the prepared MnO_x spheres as cathode materials for Li-ion batteries (LIBs)

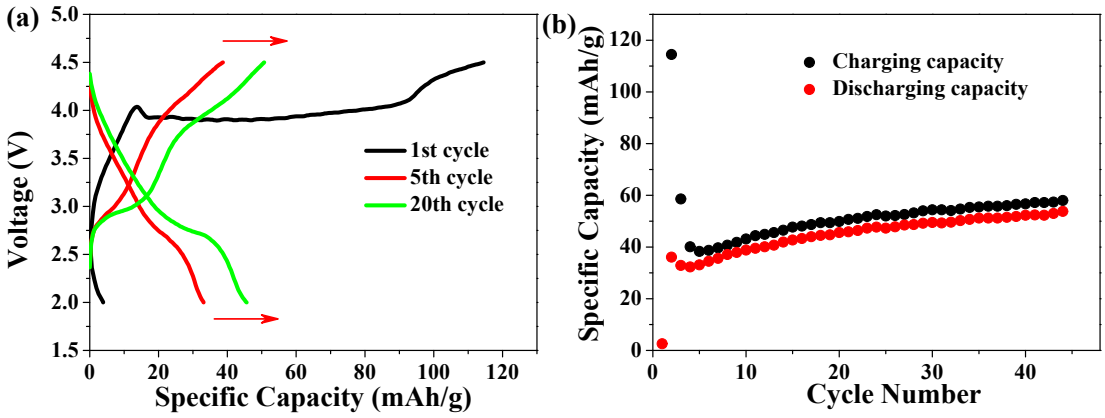

Figure S5. (a) The discharge-charge curves at a current density of 100 mA/g_{carbon} of Li-ion batteries with mixed-valent MnO_x spheres cathode at 2.0-4.5 V. (b) Cycling performance of the mixed-valent MnO_x spheres cathode.

8. Cycling performance of Li-O_2 batteries at a limited capacity of 2000 mAh/g_{carbon}

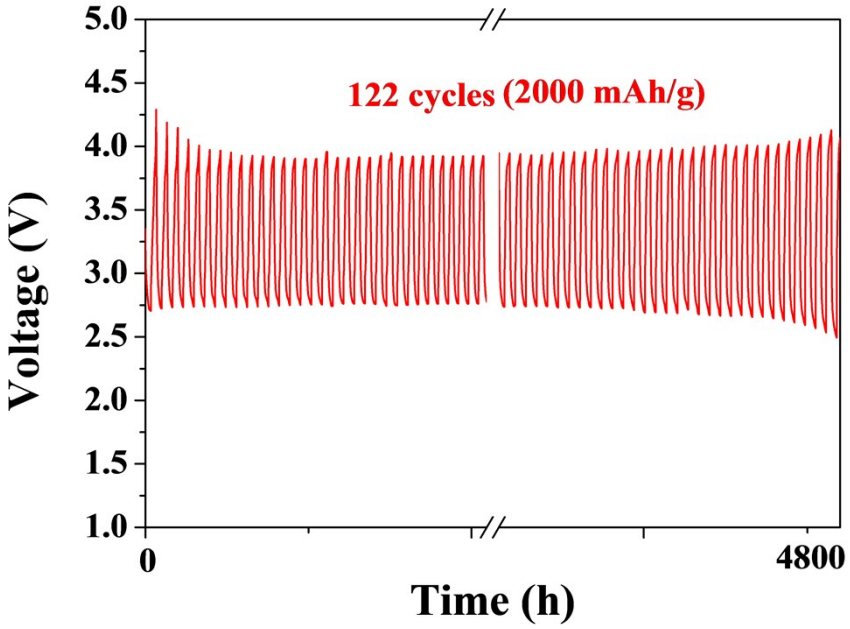

Figure S6. Cycling performance of Li-O_2 batteries with mixed-valent MnO_x spheres under 200 mA/g_{carbon} at a limited capacity of 2000 mAh/g_{carbon}.

9. HRTEM image of the Li_2O_2 shell formed on the surface of mixed-valent MnO_x spheres during discharge process

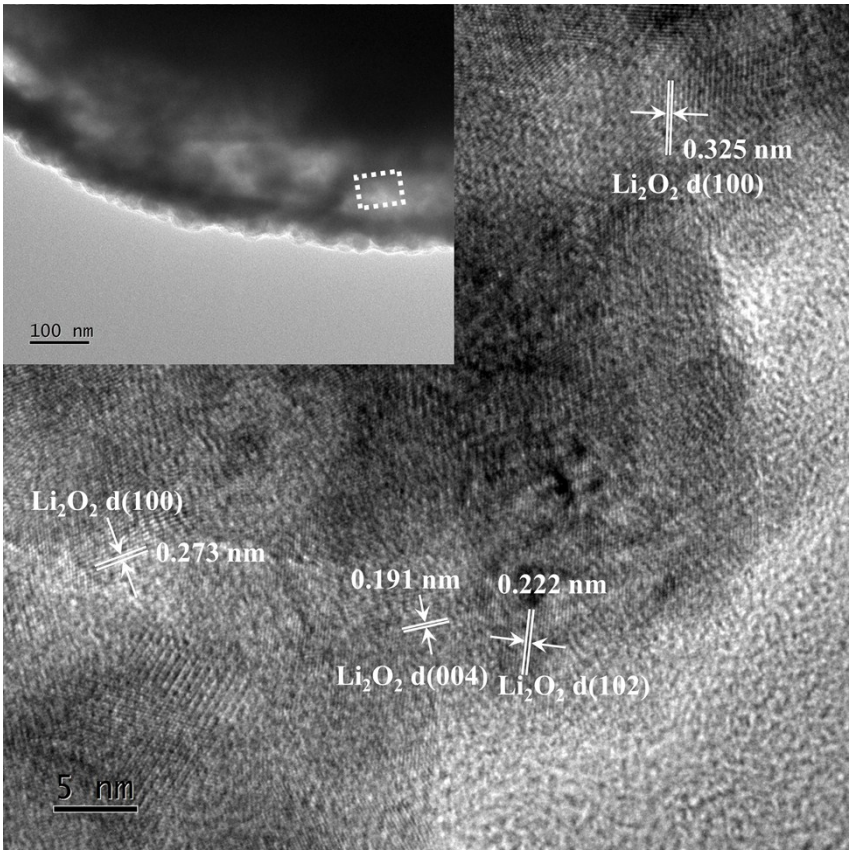

Figure S7. XRD pattern of mixed-valent MnO_x spheres electrode after first discharge and charge.

10. SEM image of the Li_2O_2 shell formed on the surface of conductive carbon during discharge process

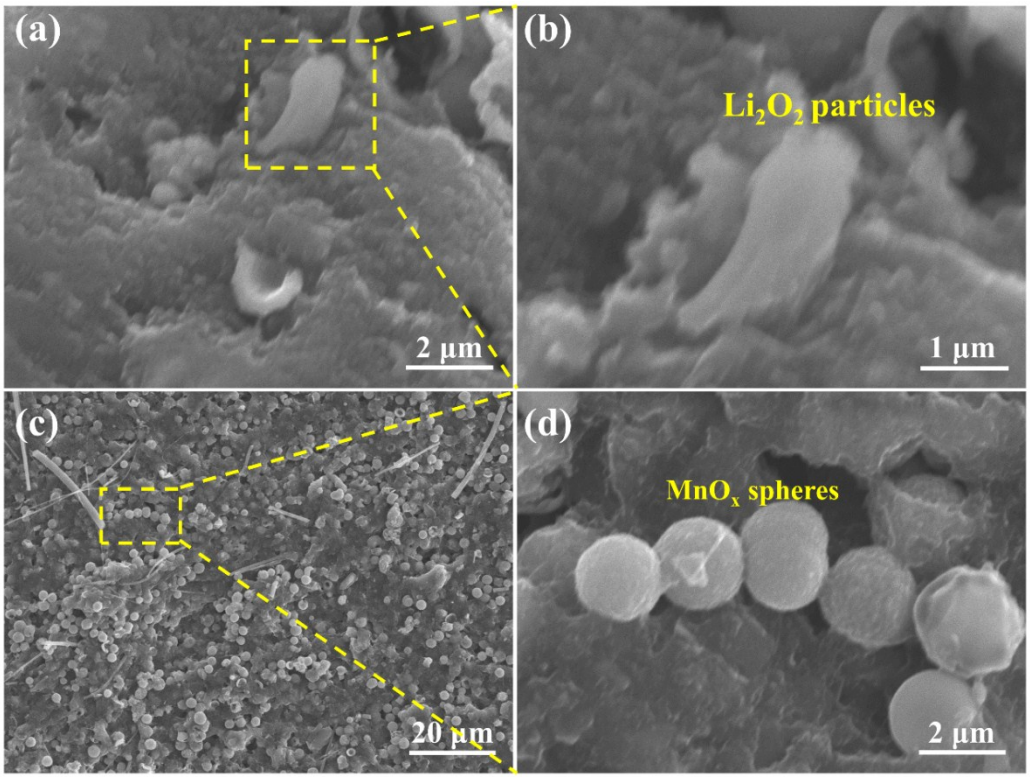

Figure S8. (a) SEM image of the MnO_x electrodes after discharging to 2.5 V. (b) Corresponding enlarged SEM image of the yellow area in (a). SEM (c) and corresponding enlarged images (d) of the MnO_x electrodes after one deep discharge-charge cycle.

11. XRD pattern of mixed-valent MnO_x spheres electrode after first discharge and charge

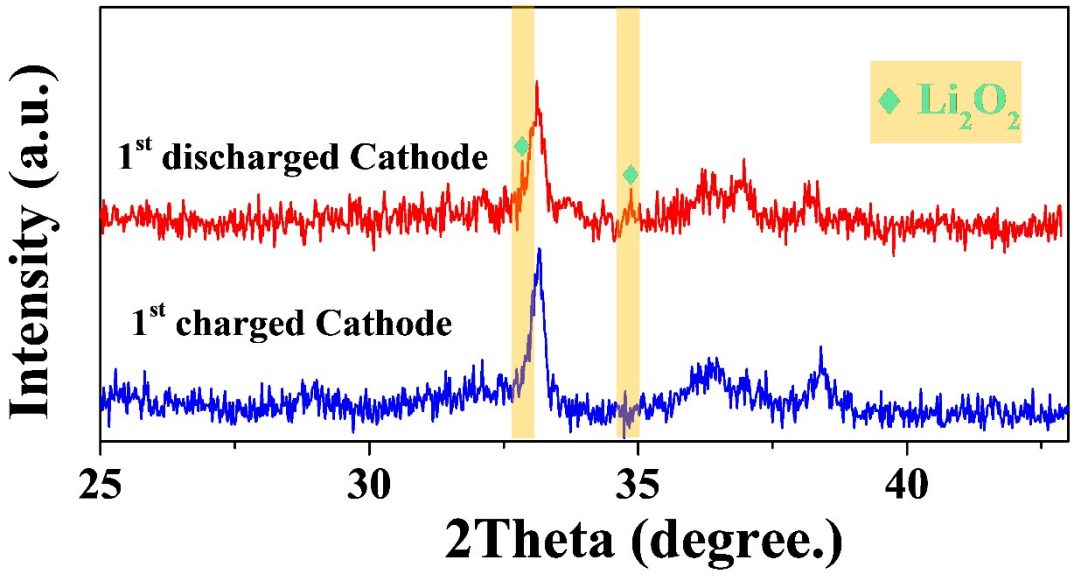

Figure S9. XRD pattern of mixed-valent MnO_x spheres electrode after first discharge and charge.

As can be seen from Figure S7, the diffraction patterns of the MnO_x show no obvious change, indicating the stability of mixed-valence state of the MnO_x. And the new diffraction peaks of the discharged MnO_x electrode appeared at 33°and 35° agree well with the standard pattern of Li_2O_2 (JCPDS card No. 73-1640). After recharging to 4.3 V, the Li_2O_2 diffraction peaks disappear, which proves the reversible formation of discharging products.